Chapter 5

Sulfur centered hydrogen bonds in methanethiol-water clusters

5.1 Introduction

Methanethiol, the sulfur analogue of methanol, is a well-known active astrochemical compound found in the interstellar medium [118]. It is also found in the blood, brain, and feces of animals and humans besides being found in plant tissues and on the surface of seawater [152]. Continuing the investigations on methanethiol, in this chapter its clusters with water is taken up. Generally, methanethiol is less soluble in water than methanol at room temperature due to the smaller electronegativity of the sulfur atom. Its solubility is primarily regulated by varying the temperature, pressure, and pH [153]. All these parameters play an important role in defining the noncovalent interactions of methanethiol either with itself or with water molecules [154]. So the methanethiol-water cluster system acts like a model system to attain better understanding of the sulfur centered hydrogen bonding systems (SCHBs).

Researchers studied SCHBs and compared their strength with the conventional oxygen-centered hydrogen bonds [36,155–162]. Biswal et al. investigated O-H---O and O-H---S hydrogen bonding in complexes of the p-cresol with methanol, ethanol, methanethiol, and ethanethiol by both computational and experimental approach. They pointed out that the strength of the hydrogen bond increased with the increase in the alkyl chain length [163]. Biswal et al. further explored these two hydrogen bonds by combining experimental and computational results for complexes of p-cresol with tetrahydrofuran (THF) and tetrahydrothiophene (THT) where they reported the interaction energy corresponding to these complexes as -7.42 kcal/mol and 6.15 kcal/mol for the O-H---O and O-H---S hydrogen bonds, respectively [164]. Arunan et al. measured the rotational spectra of SCHBs using C_6H_5CCH---H_2S system and showed that the dispersive forces played a vital role in the hydrogen bonding and the SCHB bond length in this case was 3.74 Å [156].

SCHBs in the protein system were studied by Van Berger et al. and they identified the weakest-sulfur hydrogen bond responsible for the nucleophilic attacks on the cysteine moiety by hydrogen peroxide [158]. Juanes et al. further explored SCHBs by both experimental and computational tools on thenyl alcohol hydrate and thenyl mercaptan hydrate complexes. They found out that the water molecules behaved as a proton acceptor in thenyl alcohol hydrate but were proton donor in thenyl mercaptan hydrate complex [159]. Lobo et al. reported further instances in favor of SCHBs by studying 2-phenylethanethiol (PET)−water cluster and PET−diethyl ether cluster where O-H---S and S-H---O type of interactions were identified, respectively [165]. Arnav et al. reported donor behavior of the sulfur atom in the hydrated complex of aromatic and aliphatic thiols where the interaction energy corresponding to these complexes were reported to be in the range of -2.1 kcal/mol to -3.6 kcal/mol [166] which happens to be the latest work on SCHBs.

Unlike the mixed molecular complexes based on oxygen atoms (like alcohol-water clusters) which have been a subject of continued and intense exploration ever since the discovery of hydrogen bonding, SCHBs were relatively less explored. According to the report by Mondal et al., in methanol – water clusters, it was found that the mixed cluster involving both methanol and water were found to be more stable compared to the cluster involving only methanol but less stable than cluster involving only water. They also reported that in the case of the mixed clusters, the polarizability and charge transfer were mainly responsible for the strength of the hydrogen bond, as in conventional hydrogen bonds (of clusters involving either methanol or water) [136]. Explorations of SCHBs, however little in the literature, were limited

to only the H_2S based system due to the computational ease it offered owing to its smaller size [155–157]. There exists an abject paucity of scientific literature pertaining to SCHBs using alkanethiol systems and particularly methanethiol-water systems.

Clusters of methanethiol (M) – water (W) of the type M_mW_n, where $m+n \leq 4$ with m = 0 to 4; n = 0 to 4; m and n simultaneously not being 0, are taken up for the investigation of SCHBs. The role of sulfur as both the hydrogen bond donor and acceptor in these cluster systems is extensively discussed.

5.2 Computational methods

Geometry optimization was done at B3LYP, B3LYP-D3 using aug-cc-pVNZ (where N= D, T, and Q) basis sets. Further, frequency calculations were carried out at B3LYP/cc-pVDZ and CCSD/6-311++ G(d,p) level of theory. The rationale for this theoretical preference is discussed elsewhere. Single point energies were calculated at HF, MP2, MP3, MP4, CCSD, DLPNO-CCSD(T), CCSD(T)-F12, and CCSD(T) levels of theory using cc-pVNZ (where N= D, T, Q,) and 6-311++ G(d,p) basis sets for all cluster systems and a complete basis set extrapolation was done using these values. Basis set superposition error (BSSE) correction [166] was performed at CCSD/6-311+G(d,p) level of theory. Further, natural bond orbital (NBO), Atoms in molecule (AIM) and Frontier molecular orbital (FMO) analysis were done at the B3LYP-D3/aug-cc-pVQZ level of theory. For all M_mW_n clusters and the local energy decomposition (LED) analysis was performed at DLPNO-CCSD(T)/cc-pVNZ (where N= T, Q) level of theory. Helganker method was utilized to extrapolate correlation energy, and results were obtained with basis sets cc-pVNZ (where N = T, Q) [67].

Corresponding to low energy conformers, we have performed electrostatic potential charge (ESP), non-covalent interaction (NCI) representation, atoms in Molecules (AIM) analysis, natural bond orbital (NBO) analysis and frontier molecular orbital (FMO) calculations were carried out to obtain global reactivity terms such as chemical potential (μ), hardness (η), electrophilicity index (ω), global softness (S), and electronegativity (χ) [167] were performed at the B3LYP-D3/aug-cc-pVQZ level of theory. Further, the local energy decomposition (LED) [168–172] was performed at DLPNO-CCSD(T)/cc-pVNZ (where N= T, Q) level of theory. MultiWFN software [69] was used for NCI and AIM calculations with the wave functions generated from Gaussian 16 computational suite. LED was done by using ORCA 4.2 software [146]. Gaussian 16 [68] suite of program was utilized for all other calculations.

5.3 Results and Discussion

5.3.1 Geometry

All global minimum structures of M_mW_n clusters were obtained by incorporating coordinates of global minimum structures of the homologous methanol-water clusters [136] at aforementioned levels of theory in computational method section. For global minimum structures of methanethiol cluster (M_m) we have considered conformational effect. Our previous studies already considered dimeric and trimeric cluster system of M_m where elaborate studies were done by our group; this we have done different conformational analysis for tetrameric system, which is given in Fig. 5.1.

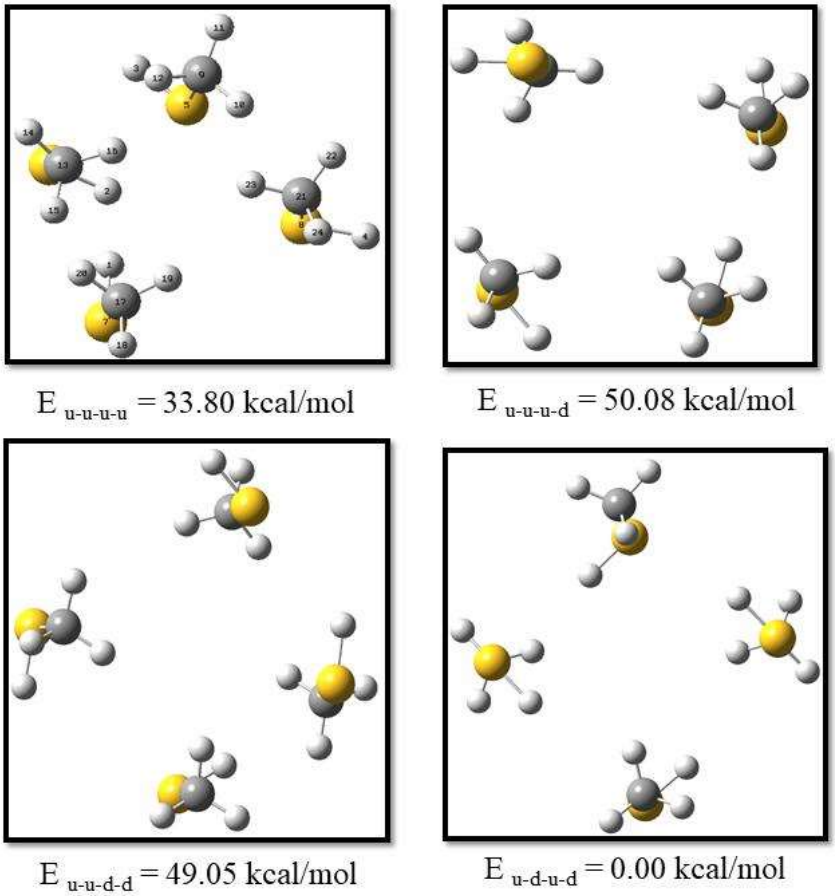

Figure 5.1 Optimized geometries at B3LYP/aug-cc-pVDZ level of theory of methanethiol clusters.

The optimized geometries of the M_mW_n clusters accommodate cyclic geometries in all modeled systems which is shown in Fig. 5.2. Dimeric systems, particularly M_2 and M_1W_1, also attain cyclic geometry through additional interaction (C-H--S in M_2 cluster and C-H--O in M_1W_1 cluster). Although these interactions fall well within the definitive limit of hydrogen bonds, their distances are comparatively larger than the S-H---S and O-H---O and interactions in the same cluster, as expected. Like dimer clusters, trimer and tetramer clusters also prefer cyclic geometries over the non-cyclic geometries because of the cooperativity phenomenon.

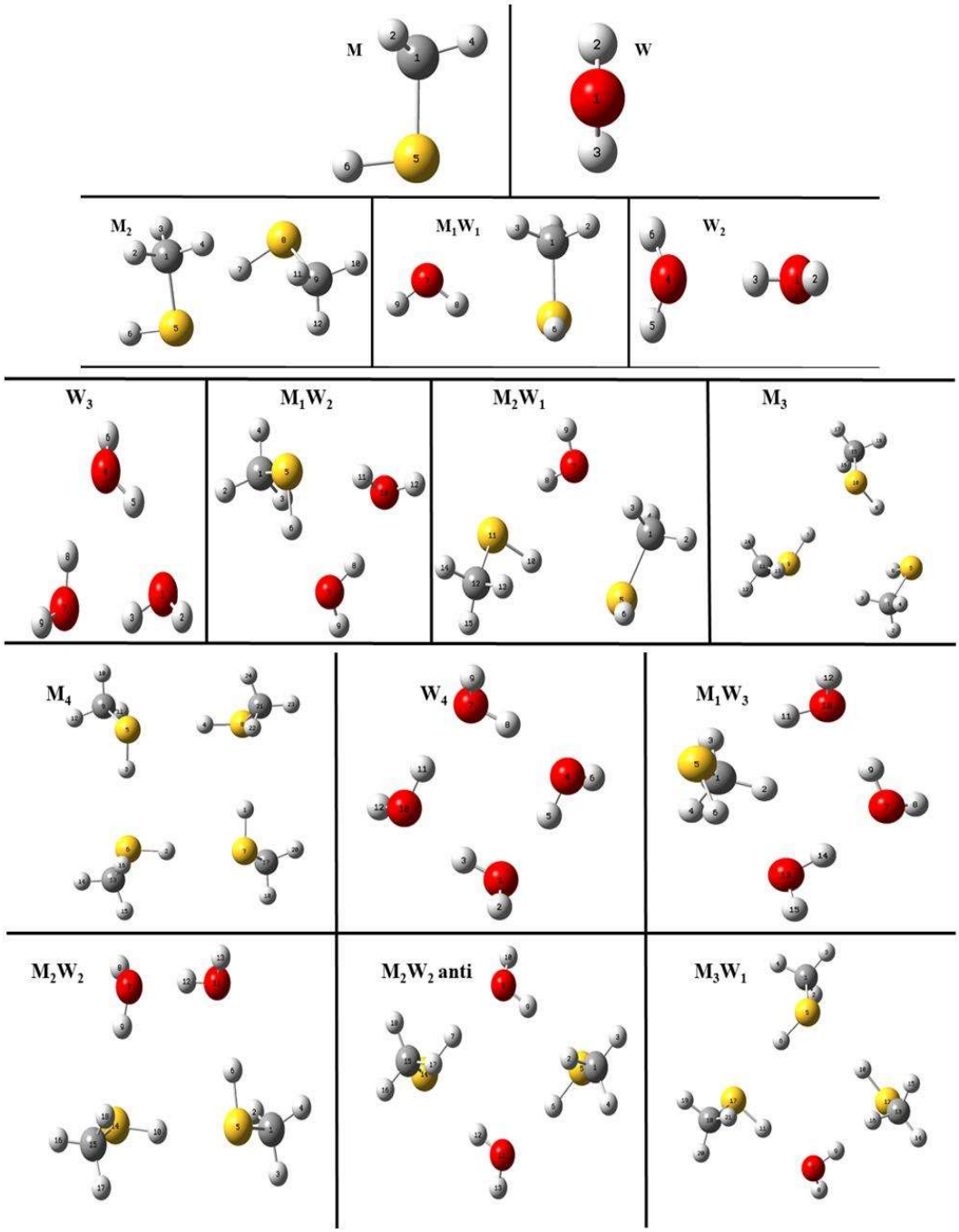

Figure 5.2 Optimized geometries at B3LYP-D3/aug-cc-pVQZ level of theory of methanethiol – water clusters: M_mW_n, where $m+n \leq 4$ with m = 0 to 4; n = 0 to 4; m and n simultaneously not being 0.

All the optimized geometries were bereft of any imaginary frequency and the summary of the normal modes of vibration corresponding to each modeled system are given in Table 5.1. This tables also compare the computed S-H and O-H vibration frequencies along with the available experimental frequencies [139,173-174]. From Table 5.1, it is evident that the normal modes vibration computed herein at B3LYP/cc-pVDZ level of theory match very well with the experiment compared to the predictions made at CCSD/6-311++G(d,p) and that of Mondal et al. [136]. From Table 5.1 we see redshift in the S-H and O-H vibrational stretching mode which was the further indication of the formation and strength of the hydrogen bonds. Hence it was inferred that the B3LYP/cc-pVDZ level of theory was the optimal computational method for studying M_mW_n clusters. This is in line with our previous findings on methanethiol molecular clusters [130].

Table 5.1 Vibrational normal modes of methanethiol - water (M_mW_n) cluster and at CCSD/6-311++G(d,p) and B3LYP/cc-pVDZ levels of theory

System	ν_{O-H} (cm^{-1})		ν_{S-H} (cm^{-1})		Experiment[1]	
	CCSD/6-311++G(d,p)[&]	B3LYP/cc-pVDZ ($$)	CCSD/6-311++G(d,p)[&]	B3LYP/cc-pVDZ	ν_{S-H} (cm^{-1})	ν_{O-H} (cm^{-1})
M	-	-	2723	2661	-	-
W	3838	3751 (3763)	-	-	-	3756
M_2	-	-	2590	2608	2601	-
	-	-	2625	2655	-	-
W_2	3750	3715 (3732)	-	-	-	3735
M_1W_1	-	3679	-	2662	-	-
	-	-	-	-	-	-
M_3	-	-	-	2570	2567	-
	-	-	-	2582	-	-
	-	-	-	2660	-	-

W_3	3614	3370 (3515)	-	-	-	3398
	3666	3483	-	-	-	3434
	3677	3488	-	-	-	3452
M_1W_2	3784	3520	2761	2502	-	-
	3816	3573	-	-	-	-
M_2W_1	3697	3608	2625	2565	-	-
	-	-	2684	2655	-	-
M_4	-	-	-	2557	2567	-
	-	-	-	2550	-	-
	-	-	-	2550	-	-
	-	-	-	2534	-	-
W_4	3436	3320 (3424)	-	-	-	3377
	3522	3421	-	-	-	3414
	3559	3460	-	-	-	3450
M_1W_3	3539	3338	2584	2375	-	-
	3587	3426	-	-	-	-
	3609	3479	-	-	-	-
M_2W_2	-	3444	-	2429	-	-
	-	3525	-	2476	-	-
M_2W_2 anti	-	3506	-	2446	-	-
	-	3521	-	2467	-	-
M_3W_1	-	3551	-	2491	-	-
	-	-	-	2513	-	-
	-	-	-	2524	-	-

Note:

1. For experimental values Ref 139, 173, and 174.
2. $$: Values in parenthesis are the predictions by Mondal et al. at B3LYP/6-311++G(d,p)
3. &: Not computed for all systems due to apparent dissimilarity with experiment as seen in the ones computed.

Further calculations were extended to different levels of theories viz. HF, B3LYP, B3LYP-D3, MP2, MP3, MP4, CCSD, CCSD(T), CCSD(T)-F12, DLPNO-CCSD(T) in order to calibrate their performance with respect to the B3LYP/cc-pVDZ level of theory. It was found that the computed results at B3LYP and B3LYP-D3 method yielded most efficient

results as compared to other methods. The geometrical parameters of M_mW_n cluster system are summarized in Table 5.2.

Table 5.2 Important geometrical parameters and interaction energies of methanethiol - water (M_mW_n) cluster systems calculated at B3LYP-D3/aug-cc-pVQZ level of theory (here numbers in parenthesis correspond to B3LYP/CBS level of theory)

System	H-X bond (not involved in H-bonding) (X = O or S or C) (Å)	H-X′ bond (involved in H-bonding) (X′= O or S or C) (Å)	H-----Y bond distance (Y= O or S) (Å)	Bond angle X-H-----Y (°)	Interaction energy (kcal/mol)
Monomer					
M	1.343	-	-	-	-
W	0.961	-	-	-	-
Dimer					
M_2	1.343 (S-H)	1.347	2.874 (S-H---S)	163.93	(-1.06) -3.39
W_2	0.961 (O-H) 0.968 (O-H) 0.960 (O-H)	0.961 (H-O)	1.956 (O-H---O)	172.40	(-4.62) -5.33
M_1W_1	0.960 (O-H) 1.343 (S-H) 1.086 (C-H)	0.968 (H-O)	2.482 (O-H---S)	158.30	(-3.26) -4.62
Trimer					
M_3	1.345 (S-H) 1.087 (C-H) 1.087 (C-H)	1.350 (S-H) 1.350 (S-H) 1.087 (C-H)	2.794 (S-H---S) 2.847 (S-H---S) 3.180 (C-H----S)	170.37 170.22 164.08	(-6.84) -8.53
W_3	0.960 (H-O) 0.960 (H-O) 0.960 (H-O)	0.975 0.974 0975	1.924 (O-H---O) 1.901 (O-H---O) 1.901 (O-H---O)	151.51 151.43 149.07	(-14.46) -16.72
M_1W_2	1.086 (C-H) 0.960 (H-O) 0.959 (H-O)	1.344 (S-H) 0.972 (H-O) 0.973 (H-O)	2.566 (S-H---O) 2.415 (O-H---S) 1.918 (O-H---O)	128.01 156.77 159.01	(-9.75) -13.07
M_2W_1	1.086 (C-H) 0.960 (H-O) 1.086 (C-H) 1.087 (C-H)	1.349 (S-H) 0.971 (H-O) 1.086 (C-H)	2.797 (S-H---S) 2.479 (C-H---O) 2.438 (O-H----S)	164.19 163.97 165.00	(-5.78) -10.09
Tetramer					
M_4	1.087 (C-H)	1.349 (S-H)	2.776 (S-H---S) 2.776 (S-H---S) 2.776 (S-H---S) 2.776 (S-H---S)	176.43 176.43 176.43 176.44	(-5.16) -14.07

W_4	0.961 (H-O)	0.984 (H-O) 0.984 (H-O) 0.984 (H-O) 0.984 (H-O)	1.770 (O-H---O) 1.770 (O-H---O) 1.770 (O-H---O) 1.770 (O-H---O)	167.50 167.49 167.51 167.49	(-20.41) -29.55
M_1W_3	1.087 (C-H) 0.960 (H-O) 0.960 (H-O) 0.960 (H-O)	1.353 (S-H) 0.978 (H-O) 0.978 (H-O) 0.977 (H-O)	2.091 (S-H---O) 1.825 (O-H---O) 1.809 (O-H---O) 2.342 (O-H---S)	165.82 170.85 170.60 168.63	(-18.97) -23.15
M_2W_2	1.087 (C-H) 1.087 (C-H) 0.960 (H-O) 0.961 (H-O)	1.353 (S-H) 1.351 (S-H) 0.975 (H-O) 0.975 (H-O)	2.676 (S-H---S) 2.140 (S-H---O) 1.853 (O-H---O) 2.366 (O-H---S)	168.96 170.62 173.11 171.68	(-13.56) -19.96
M_2W_2 anti	1.096 (C-H) 0.964 (H-O) 1.096 (C-H) 0.964 (H-O)	1.365 (S-H) 0.979 (H-O) 1.365 (S-H) 0.979 (H-O)	2.094 (S-H---O 2.354 (O-H---S 2.095 (S-H---O 2.354 (O-H---S)	168.66 170.96 168.78 171.03	(-11.80) -17.56
M_3W_1	1.087 (C-H) 1.087 (C-H) 1.087 (C-H) 0.962 (H-O)	1.351 (S-H) 1.353 (S-H) 1.353 (S-H) 0.973 (H-O)	2.721 (S-H---S) 2.709 (S-H---S) 2.412 (O-H---S) 2.184 (S-H---O)	174.34 172.07 172.95 173.27	(-8.55) -15.82

Computed distances corresponding to hydrogen bonds like O-H---O, S-H---O, S-H---S, and O-H---S were in the range of 1.90 Å to 3.20 Å in all clusters systems (M_m, W_n, and M_mW_n). The S-H--S bond distance in the case of all methanethiol cluster system was found to be between 3 Å and 4 Å [130]. Similarly, the O-H--O bond distance was seen to be in the range 1.74 Å to 1.95 Å in the case of methanol-water cluster system [136]. The distance range computed herein lay within the limits prescribed for other unconventional hydrogen bonds [26] as well. The O-H and S-H distances in bare water and methanethiol molecule is 0.961 Å and 1.343 Å respectively. When water molecule interacts with methanethiol, then both the S-H and the O-H bonds get enlarged. The OH bonds were seen enlarged from 0.001 Å to 0.029 Å and correspondingly the SH bonds were seen enlarged from 0.002 Å to 0.022 Å in different cluster systems.

The hydrogen bond distance corresponding to S-H---O, S-H---S, O-H---O, and O-H---S bonds vary like S-H---S>O-H---S>S-H---O>O-H---O, as inferred from Table 5.1 and this was consistent in all the cluster systems studied herein. Overall there were in total 39 instances of hydrogen bonds observed by considering all the cluster systems. Of these, there were 6 instances of S-H---O, 12 instances of S-H---S, 12 instances of O-H---O and 8 instances of O-H---S hydrogen bonds. Alongside, there also exists hydrogen bonds of the type C-H---O and C-H---S in M_2W_1 and M_3 cyclic systems, respectively, with significant energies although not as high as the other hydrogen bonds.

Conventionally, sulfur atom acts as a donor partner for hydrogen bonds and to revert the change it requires some substitution. There were 8 instances of O-H---S type hydrogen bonds in M_mW_n clusters where they play a significant role in stabilization of the cluster. Generally, distances are smaller for strong hydrogen bonds but it was found that the O-H---S hydrogen bond was stronger and larger (-4.27 kcal/mol; 2.566 Å) compared to the S-H---O hydrogen bond (-4.57 kcal/mol; 2.438 Å). This could be due to the better overlapping of the lone pair of sulfur atom and antibonding orbital of the O-H bond in their cyclic structure. This was also confirmed by the NBO and AIM analysis and shown in Table 5.6. For M_mW_n clusters, the distances corresponding to S-H---O, S-H---S, O-H---O, and O-H---S hydrogen bonds lie in between the values corresponding to the distances in methanethiol-only and water-only clusters. Similar trend was also reported for the methanol-water system of Mondal et al. [136].

Table 5.3 Comparison of interaction energies (IE) of M_mW_n clusters at various methods (all values in kcal/mol)

System↓ / methods →	B3LYP/CBS	B3LYP-D3/CBS	DLPNO-CCSD(T)/CBS	CCSD-F12/CBS	(CCSD/cc-pVDZ) BSSE Corrected interaction energy
M_2	-1.06	-3.39	-3.92	-0.89	-1.73
W_2	-4.62	-5.33	-7.06	-5.72	-4.19
M_1W_1	-3.26	-4.62	-5.05	-3.35	-3.24
M_3	-6.84	-8.53 (-1.64)	-8.98	-1.52	-4.41
W_3	-14.46	-16.72 (-2.03)	-22.57	-17.23	-13.38
M_1W_2	-9.75	-13.07 (-1.50)	-16.48	-11.37	-9.68
M_2W_1	-5.78	-10.09 (-2.53)	-12.21	-6.46	-6.48
M_4	-5.16	-14.07 (-6.27)	-13.96	-0.38	-4.85
W_4	-20.41	-29.55 (-4.54)	-38.09	-28.94	-23.01
M_1W_3	-18.97	-23.15 (-5.05)	-29.37	-20.69	-17.58
M_2W_2	-13.56	-19.96 (-7.23)	-25.06	-14.90	-13.28
M_2W_2 (anti)	-11.80	-17.56 (-8.20)	-20.23	-14.46	-12.02
M_3W_1	-8.55	-15.82 (-9.63)	-18.67	-7.71	-9.66

Note: 1. $IE = E_{cluster} - (\sum_{m=1}^{4} E_{Mm} + \sum_{n=1}^{4} E_{Wn})$
2. Values in parenthesis shows cooperativity energy

Interaction energy (IE) (given in Tables 5.2, 5.3, and 5.4) corresponding to the dimer systems was found to be in the range from -3.38 to -5.33 kcal/mol, for trimer the IE was found to be in the range from -8.52 to -10.09 kcal/mol, and for tetramer the range of IE was from -14.07 to -17.56 kcal/mol. All these values are well within the acceptable range for hydrogen bonding system [26]. According to Sheng et al., BSSE correction is not useful for short range or Van der Waals distances [175].

Table 5.4 CBS limit, single point interaction energy (IE[&]) of M_mW_n at different levels of theory (all values in kcal/mol)

System/Method	HF	MP2	MP3	MP4	CCSD	CCSD(T)
Dimer						
M_2	-3.33	-2.94	-2.46	-2.40	-2.20	-2.56
W_2	-3.51	-5.07	-4.95	-4.91	-4.79	-5.07
M_1W_1	-3.36	-4.32	-3.92	-3.90	-3.70	-4.12
Trimer						
M_3	-4.06	-6.43	-5.35	-5.37	-4.72	-5.90
W_3	-10.04	-15.98	-15.38	-15.32	-14.89	-15.94
M_1W_2	-7.65	-12.31	-11.42	-11.39	-10.95	-12.66
Tetramer						
M_1W_3	-13.48	-22.07	-20.63	-20.55	-19.76	-21.54
M_2W_2	-10.42	-17.78	-16.14	-16.04	-15.18	-16.95
& Note: $IE = (E_{cluster} - (\sum_{m=1}^{4} M_m + \sum_{n=1}^{4} W_n))$						

The M_mW_n cluster systems in a way testify this statement as the BSSE corrected interaction energy of the M_mW_n clusters at CCSD/cc-pVDZ level of theory was very much similar to the extrapolated B3LYP/CBS level of theory (Table 5.3) indicating the cancelation of the BSSE. Hence for the modeled systems studied herein the BSSE correction was not required. Similar to the report of Mondal et al. [136], the interaction energies of M_mW_n lie in between water-only and methanethiol-only cluster system. Interaction energy per hydrogen bond for dimer (M_1W_1), trimer (M_1W_2), and tetramer (M_1W_3) clusters were in between -3.25 and -4.74 kcal/mol. This was also the case for clusters like M_2W_1, M_2W_2, and M_2W_2 anti. Per hydrogen bond for M_3W_1 clusters was around 4 kcal/mol. Value of per hydrogen bond for W_n and M_m cluster was seen to monotonously increase from dimer to tetramer, clearly indicating

the cooperativity effect in play in the modeled systems as given in Tables 5.3. Cooperativity effect increases as the cluster size increases consequence of this the strength of the hydrogen bonding is enhanced.

Stabilization generally enhanced with the incorporation of water molecules along with methanethiol. Whereas it was found that M_1W_3 cluster (interaction energy -23.15 kcal/mol) was the most stable cluster followed by M_2W_2 (interaction energy = -19.96 kcal/mol), in the case of methanol-water clusters the $(MOH)_3W_1$ system was the most stable one followed by the $(MOH)_1W_3$ system. In the M_4 cluster when one M is replaced by a W, the overall energy of the cluster got further stabilized by 1 kcal/mol. Similarly going from M_3W_1 cluster system to M_2W_2, the cluster got additionally stabilized by 4 kcal/mol and similar was the case when moving from M_2W_2 to M_1W_3.

5.3.2 Local energy decomposition (LED) analysis

Different contributing factors for the interaction energy of the modeled system were obtained with the help of local energy decomposition (LED) calculations. LED analysis was carried out using the ORCA computing suit where the contribution to interaction energy was through two factors i.e., reference energy and correlation energy. Further, reference energy was split into three energy terms i.e., electrostatic interaction energy (attractive), electronic preparation energy (repulsive and it is the energy that is required for a molecule to be in close proximity so that interactions take place, and counters the effect of the electrostatic interactions) and electron exchange interaction (attractive) [166]. LED incorporates dispersive effects in correlation energy, and further, it is decomposed into strong and weak pair

contributions along with triple corrections. The simplified values of the interaction energies in M_mW_n are given in Table 5.5.

Table 5.5 Local energy decomposition (LED) of methanethiol - water (M_mW_n) clusters at DLPNO-CCSD(T)/cc-pVTZ level of theory. (All energies in kcal/mol)

System	ΔE_{int}	ΔE_{int}^{ref}	ΔE_{el-pre}^{ref}	ΔE_{elstat}	ΔE_{exch}	ΔE_{int}^{C}	ΔE_{int}^{C-SP}	ΔE_{int}^{C-W}	$\Delta E_{int}^{C-(T}$
Dimer									
M_2	-4.82	-1.76	15.33	-13.33	-3.76	-3.06	-2.70	-0.03	-0.33
W_2	-7.31	-5.6	23.33	-24.84	-4.05	-1.75	-1.54	-0.01	-0.20
M_1W_1	-5.70	-3.36	23.08	-21.99	-4.45	-2.34	-2.07	-0.02	-0.25
Trimer									
M_3	-10.54	-2.48	53.27	-44.65	-11.10	-8.06	-7.02	-0.16	-0.88
W_3	-23.55	-17.07	88.65	-91.17	-14.55	-6.48	-5.71	-0.04	-0.73
M_1W_2	-17.72	-11.57	69.70	-68.97	-12.30	-6.15	-5.43	-0.05	-0.67
M_2W_1	-13.47	-6.96	57.14	-53.09	-11.01	-6.52	-5.72	-0.09	-0.71
Tetramer									
M_4	-16.01	-1.42	93.94	-75.99	-19.38	-14.59	-12.68	-0.33	-1.58
W_4	-40.17	-28.29	183.00	-183.47	-27.82	-11.87	-10.39	-0.18	-1.30
M_1W_3	-31.08	-20.21	143.24	-140.05	-23.40	-10.87	-9.53	-0.15	-1.19
M_2W_2	-26.97	-15.19	127.85	-120.52	-22.52	-11.78	-10.34	-0.13	-1.30
M_2W_2 anti	-21.81	-13.16	109.80	-140.37	-18.59	-8.65	-7.38	-0.35	-0.92
M_3W_1	-20.60	-8.39	109.80	-97.64	-20.55	-12.21	-10.58	-0.30	-1.33

From Table 5.5, it is evident that electrostatic > exchange > strong pair > weak pair correlation energy in all the M_mW_n clusters, making the electrostatic correlation energy as the most dominating contributor in all the modeled systems.

5.3.3 Atoms in Molecules (AIM) analysis

Various properties and forces involved in the molecular cluster system is well decoded by the distribution electron densities throughout the whole system. In this context, Laplacian electron density and total electron density play crucial role in the assessment of the inter or intra molecular interactions. Majorly, the electron density ($\rho(r)$) and Laplacian ($\nabla^2\rho(r)$) play a significant role in characterizing the hydrogen bond thus we completed AIM calculations for our system to clarify the precise nature of the interactions [175]. As per the Koch and Popelier predictions, bond critical points (BCP) elucidate the path of the hydrogen bonds where the value of $\rho(r)$ lie in the range from 0.002 to 0.040 a.u. and $\nabla^2\rho(r)$ in the range from 0.024 to 0.139 a.u. [73, 130, 139, 175]. The calculated parameters of BCP of (3, -1) are given in Table 5.6, and their corresponding basin surfaces are shown in Fig. 5.3.

Table 5.6 Topological parameters for bonds of interacting atoms in methanethiol (M) – water (W) clusters: electron density (ρ), Laplacian of electron density ($\nabla^2\rho$), kinetic electron energy density (G_{BCP}), potential electron energy density (V_{BCP}), total electron energy density (H_{BCP}), estimated interaction energy (E_{int}) at bond critical points (BCP) at B3LYP-D3/aug-cc-pVQZ level of theory

	BCP number	ρ	$\nabla^2\rho_{BCP}$	G_{BCP}	V_{BCP}	H_{BCP}	E_{int}
Dimer							
M_2	4 (S-H--S)	0.0089	0.0205	0.0044	-0.0037	0.0007	-1.18
W_2	4 (O-H--O)	0.0247	0.0784	0.0197	-0.0197	-0.0001	-6.21
M_1W_1	3 (O-H--S)	0.0131	0.0609	0.0142	-0.0131	0.0010	-4.12
Trimer							
M_3	6 (S-H--S)	0.0090	0.0211	0.0050	-0.0047	0.0003	-1.48
	14 (S-H--S)	0.0073	0.0175	0.0040	-0.0036	0.0004	-1.14
	15 (S-H--S)	0.0085	0.0206	0.0048	-0.0045	0.0003	-1.40
W_3	2 (O-H--O)	0.0270	0.0851	0.0219	-0.0225	-0.0006	-7.08
	7 (O-H--O)	0.0289	0.0883	0.0232	-0.0242	-0.0011	-7.63
	8 (O-H--O)	0.0287	0.0887	0.0232	-0.0242	-0.0010	-7.61
M_1W_2	3 (O-H--S)	0.0197	0.0381	0.0105	-0.0114	-0.0010	-3.60
	6 (O-H--O)	0.0272	0.0845	0.0218	-0.0224	-0.0006	-7.05

	12 (S-H--O)	0.0072	0.0285	0.0055	-0.0038	0.0016	-1.21
M_2W_1	6 (S-H--S)	0.0105	0.0232	0.0052	-0.0045	0.0006	-1.42
	10 (O-H--S)	0.0186	0.0368	0.0099	-0.0106	-0.0007	-3.33
	15 (C-H--O)	0.0085	0.0308	0.0062	-0.0047	0.0015	-1.47
Tetramer							
M_4	7 (S-H--S)	0.0109	0.0237	0.0053	-0.0047	0.0006	-1.48
	12 (S-H--S)	0.0109	0.0237	0.0053	-0.0047	0.0006	-1.48
	13 (S-H--S)	0.0109	0.0237	0.0053	-0.0047	0.0006	-1.48
	15 (S-H--S)	0.0109	0.0237	0.0053	-0.0047	0.0006	-1.48
W_4	3 (O-H--O)	0.0383	0.1069	0.0301	-0.0335	-0.0034	-10.55
	4 (O-H--O)	0.0383	0.1069	0.0301	-0.0335	-0.0034	-10.55
	10 (O-H--O)	0.0383	0.1069	0.0301	-0.0335	-0.0034	-10.55
	11 (O-H--O)	0.0383	0.1069	0.0301	-0.0335	-0.0034	-10.55
M_1W_3	3 (O-H--S)	0.0231	0.0403	0.0118	-0.0136	-0.0017	-4.27
	4 (O-H--O)	0.0351	0.1022	0.0279	-0.0302	-0.0023	-9.50
	13 (O-H--O)	0.0341	0.0992	0.0269	-0.0290	-0.0021	-9.13
	14 (S-H--O)	0.0103	0.0626	0.0151	-0.0145	0.0006	-4.56
M_2W_2	7 (S-H--S)	0.0133	0.0273	0.0064	-0.0061	0.0004	-1.91
	12 (O-H--S)	0.0219	0.0395	0.0113	-0.0127	-0.0014	-4.01
	14 (S-H--O)	0.0185	0.0574	0.0134	-0.0125	0.0009	-3.94
	16 (O-H--O)	0.0315	0.0947	0.0251	-0.0265	-0.0014	-8.30
M_2W_2 (anti)	5(O-H--S)	0.0229	0.0417	0.0121	-0.0137	-0.0017	-4.31
	3(S-H--O)	0.0196	0.0614	0.0145	-0.0136	0.0009	-4.27
	19(O-H--S)	0.0229	0.0417	0.0121	-0.0137	-0.0017	-4.31
	20(S-H--O)	0.0196	0.0614	0.0145	-0.0136	0.0009	-4.27
M_3W_1	5 (S-H--O)	0.0164	0.0558	0.0119	-0.0099	0.0020	-3.11
	8 (O-H--S)	0.0200	0.0391	0.0108	-0.0118	-0.0010	-3.71
	16 (S-H--S)	0.0121	0.0265	0.0060	-0.0054	0.0006	-1.69
	17 (S-H--S)	0.0124	0.0271	0.0061	-0.0055	0.0006	-1.74

For the systems studied herein, it was found that both the $\nabla^2\rho(r)$ and $\rho(r)$ exhibited the following trend for the O-H---O > S-H---S > O-H---S > S-H---O hydrogen bonds. This sequence generally depends upon the transfer of electron density from donor to acceptor moieties of the respective interaction.

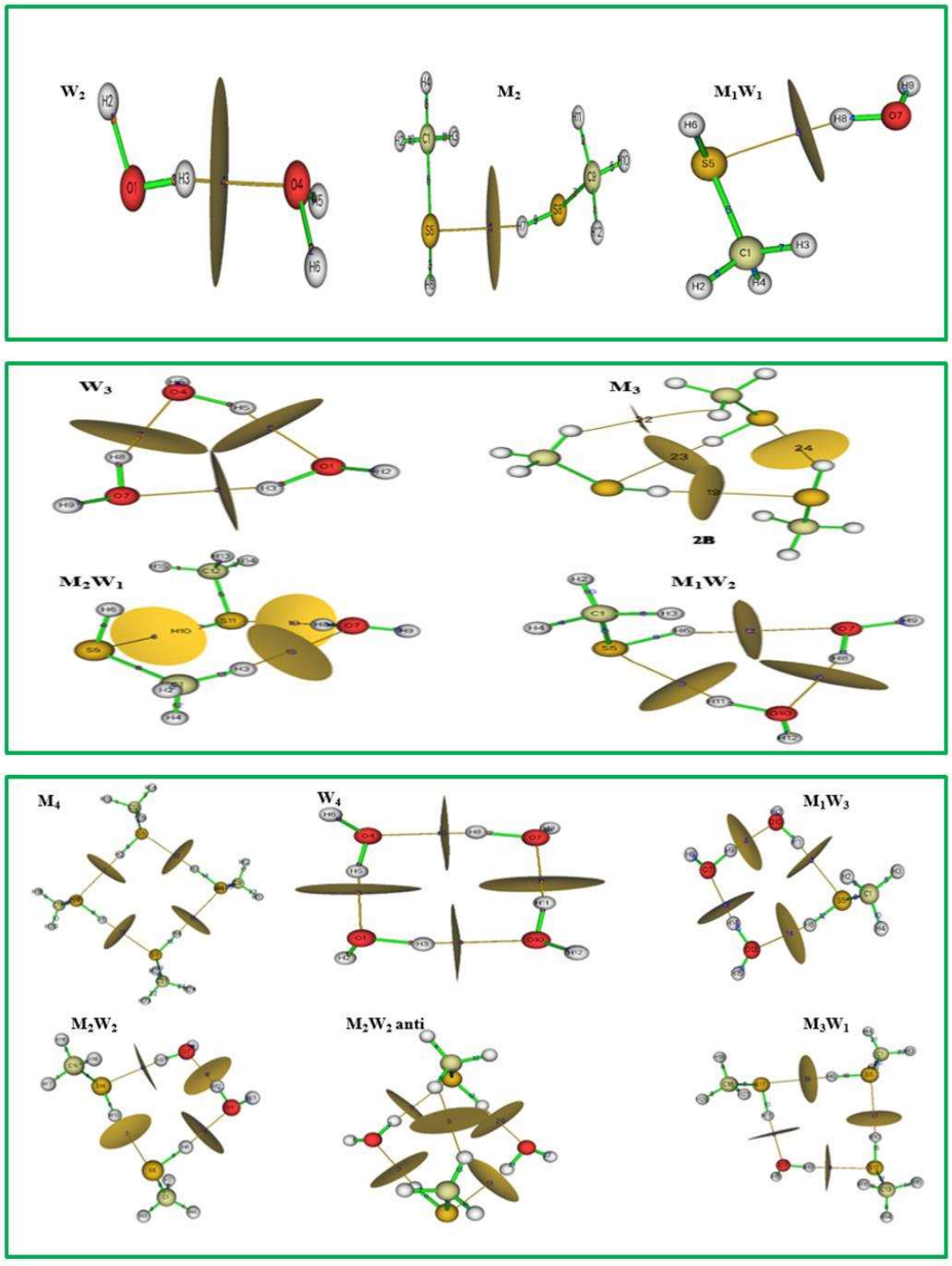

Figure 5.3 Inter-basin surfaces for methanethiol - water (M_mW_n) clusters at AIM/B3LYP-D3/aug-cc-pVQZ.

The computed results for the systems modelled herein were seen to follow the conditions of Rozas et al. [33] very well for all the SCHB interactions, once again reinforcing the weak and electrostatic nature of these interactions. This prediction also depends on the amount of transfer of electron density between the moieties involved. Further, the interaction energy at all possible BCPs was calculated for all M_mW_n clusters using the method ($E_{int} = ½V$; where V = potential electron energy density) described by Espinosa et al. [72], and it was found that the obtained interaction energies were higher for water-only clusters followed by mixed clusters and lowest for methanethiol-only clusters. This trend of the interaction energy was seen to be consistent in different levels of theory [Refer Tables 5.3 and 5.4] and previously reported homologous molecular system [136] of the methanol-water clusters. Whereas in the case of O-H---O hydrogen bond there exist a strong correlation between Laplacian electron density and interaction energy (this work), shown in Fig. 5.4, as was also seen by Mondal et al. [136], absolutely no such correlation was seen in the case of S-H---S, O-H---S, and S-H---O hydrogen bonds due to the nature of the sulfur atom.

5.3.4 Frontier Molecular Orbital (FMO)

With the help of FMO calculations the kinetic and thermodynamic stability of the cluster systems in terms of HOMO-LUMO (H-L) gaps was estimated. Generally, the H-L gap measures s system's stability in terms of chemical hardness or global softness. Hardness of a system is linearly dependent on the values of the H-L gaps [167]. The Computed results of different energy parameters of the FMO analysis are given in Table 5.7. Usually Higher H-L gaps is the indication of the softness and global hardness of the system. For modeled system

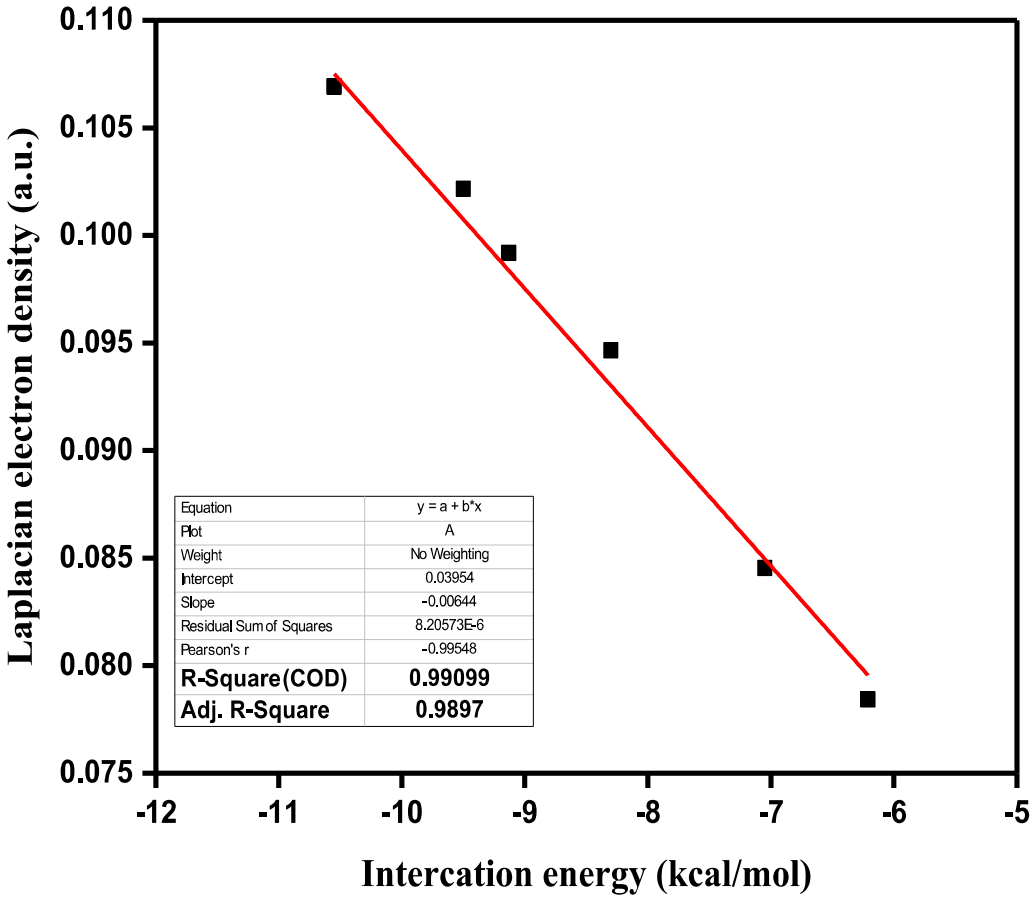

Figure 5.4 Correlation between Laplacian electron density and Interaction energy for O-H---O hydrogen bond of methanethiol -water (M_mW_n) mixed cluster system at B3LYP-D3/aug-cc-pVQZ level of theory.

of methanethiol-water cluster we found best correlation in between H-L gaps and hardness of the system as shown in Fig. 5.5. The H-L gaps for the water-only cluster were much larger (see Table 5.7), implying that the water cluster was the most stable compared to methanethiol-only and mixed clusters. The H-L gaps as well as the global softness for M_mW_n were smaller than the W_n and comparable to the M_m clusters and the same is shown in Fig. 5.6. FMO predictions justified by the NBO analysis for all the M_mW_n clusters and further FMO

analysis reinforced the findings very well (for detailed elaboration refer supplementary information).

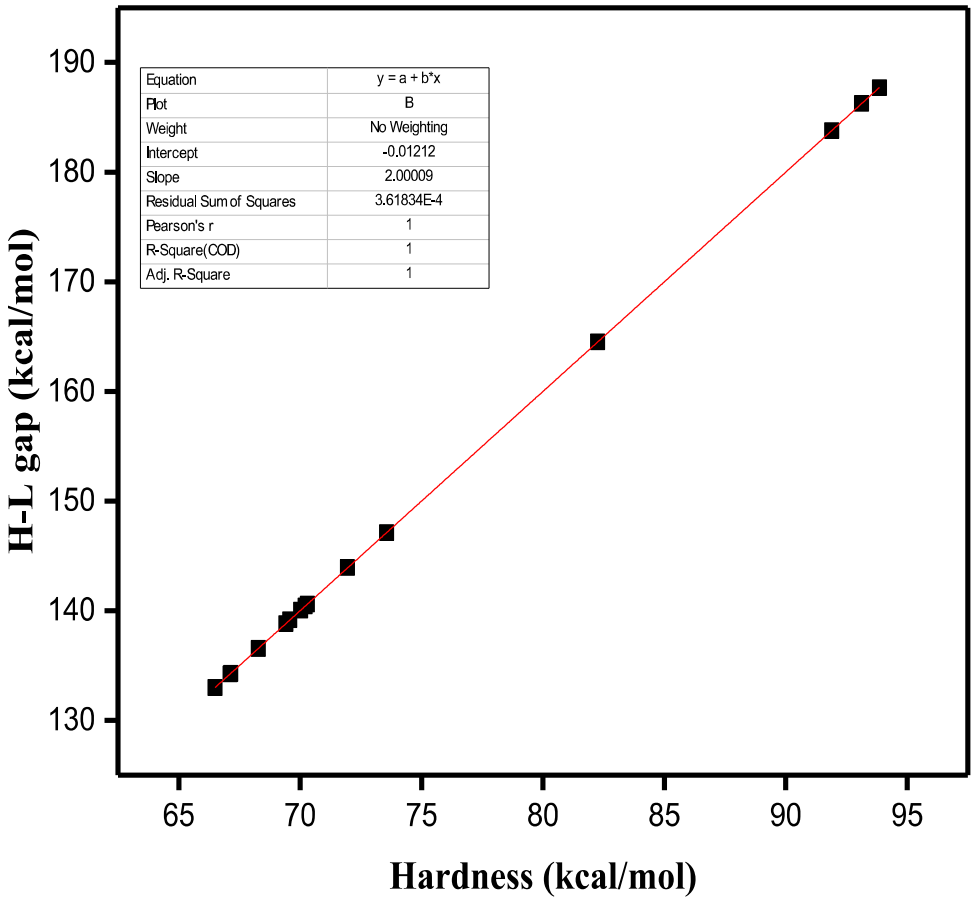

Figure 5.5 Correlation between H-L gap and hardness of the M_mW_n clusters at B3LYP/aug-cc-pVQZ level of theory.

Table 5.7 Calculated energy parameters: chemical potential (μ), hardness (η), electrophilicity index (ω), electronegativity (χ), and softness (S) and dipole moment (μ' in Debye (D)) for M_mW_n clusters at B3LYP-D3/aug-cc-pVQZ level of theory. (All energy values in kcal/mol)

System	HOMO	LUMO	H-L gap	η	S	μ	χ	ω	μ_m (D)
Dimer									
W_2	-182.80	256.54	439.34	219.67	0.005	36.87	-36.87	3.09	2.57
M_2	-154.31	81.49	235.80	117.90	0.008	-36.41	36.41	5.62	1.41
M_1W_1	-167.86	77.89	245.75	122.88	0.008	-44.99	44.99	8.23	0.58
Trimer									
W_3	-270.43	275.47	545.90	272.95	0.004	2.52	-2.52	0.01	1.11
M_3	-158.19	83.44	251.00	120.82	0.008	-37.38	37.38	5.78	1.49
M_1W_2	-168.57	82.43	136.6	125.50	0.008	-43.07	43.07	7.39	0.95
M_2W_1	-151.06	-14.46	241.63	68.30	0.015	-82.76	82.76	50.14	1.52
Tetramer									
W_4	-294.82	269.56	564.38	282.19	0.004	-12.63	12.63	0.28	0.00
M_4	-161.78	88.78	249.88	125.28	0.008	-36.5	36.5	5.32	0.00
M_1W_3	-156.59	-16.43	140.16	70.08	0.014	-86.51	86.51	53.40	1.25
M_2W_2	-148.25	-16.99	131.26	65.63	0.015	-82.62	82.62	52.00	2.76
M_2W_2 anti	-155.25	-14.80	140.45	70.23	0.014	-85.03	85.03	51.47	0.53
M_3W_1	-154.95	85.41	240.36	120.18	0.008	-34.77	34.77	5.03	2.67

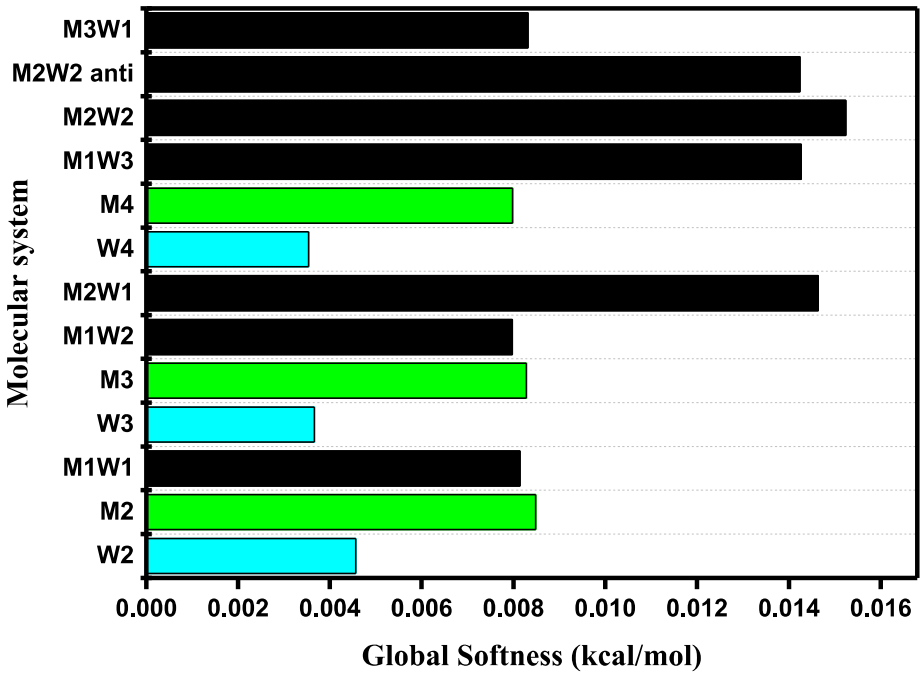

Figure 5.6 Global softness of different molecular clusters of M_mW_n cluster system at B3LYP-D3/aug-cc-pVQZ level of theory.

5.3.5 Natural bond orbital (NBO)

Methanethiol generally shows both i.e. intramolecular and intermolecular interaction because of the better availability of the lone-pair electron of the sulfur atom. Consequence of this appear in the form of the strength of the intermolecular interactions. Generally lone-pair of the sulfur atom interacts with hydrogens of the carbons atoms. So, the donation capacity of sulfur atom during intermolecular interaction is slightly reduced compared to the conventional hydrogen bonds. NBO results for methanethiol-water based clusters are given in Table 5.8. The E(2) energy corresponding to M_2, M_1W_1, and W_2 clusters are [n(S5)→ σ*H7-S8] = 1.56 kcal/mol, [n(S5)→ σ*O7-H8] = 5.29 kcal/mol, and [n(O4)→ σ*O1-H3] = 7.73 kcal/mol respectively. In dimer clusters have one hydrogen bond interaction, but the extent of charge

transfer is different and highest for W_n, and moderate for M_mW_n and weaker in the M_m cluster. This is happening because of the donor and acceptor's charger shuffling capacity. In the case of trimer and tetramer clusters, a similar variation was observed in values of the E(2) as shown in Table 5.8.

NBO analysis confirms the existence of S-H---S, S-H---O, O-H---S, and O-H---O interactions. Out of these four interactions the O-H---O interaction is more stable whereas the S-H---S interaction is least in stabilization energy but the other two interactions i.e. S-H---O, O-H---S attain moderate stabilization energy. NBO analysis clearly shows that the E(2) values are increasing continuously from dimer to tetramer clusters. NBO analysis supports the discussions in the preceding sections that the cluster attains stabilization with the size of the cluster size and flexibility of the cluster structure. Thus, natural bond orbital (NBO) calculations for all the M_mW_n clusters further reinforced the findings very well.

Table 5.8 NBO analysis at B3LYP-D3/aug-cc-pVQZ level of theory.

System	Orbital interaction	E(2) (kcal/mol)	E(j)-E(i) (a.u.)	F(i,j) (a.u.)
M_2	$LP(2)S_5 \rightarrow \sigma^*_{H7 - S8}$	1.56	0.46	0.024
W_2	$LP(2)O_4 \rightarrow \sigma^*_{O1 - H3}$	7.73	0.94	0.076
M_1W_1	$LP(2)S_5 \rightarrow \sigma^*_{O7 - H8}$	5.29	0.70	0.055
M_3	$LP(2)S_5 \rightarrow \sigma^*_{H8 - S10}$	2.78	0.45	0.032
	$LP(2)S_9 \rightarrow \sigma^*_{S5 - H6}$	2.53	0.46	0.031
	$LP(2)S_{10} \rightarrow \sigma^*_{H7 - S9}$	3.49	0.45	0.036
W_3	$LP(2)O_1 \rightarrow \sigma^*_{O4 - H5}$	9.23	0.87	0.080
	$LP(2)O_4 \rightarrow \sigma^*_{O7 - H8}$	9.43	0.85	0.080
	$LP(2)O_7 \rightarrow \sigma^*_{O1 - H3}$	8.16	0.87	0.075
M_1W_2	$LP(2)S_5 \rightarrow \sigma^*_{O7 - H9}$	0.07	0.72	0.006
	$LP(2)S_5 \rightarrow \sigma^*_{O10 - H11}$	8.81	0.68	0.069
	$LP(1)S_5 \rightarrow \sigma^*_{O10 - H11}$	0.18	1.03	0.012
	$LP(1)O_7 \rightarrow \sigma^*_{S5 - H6}$	0.37	0.82	0.016
	$LP(2)O_{10} \rightarrow \sigma^*_{O7 - H8}$	9.24	0.88	0.081

M_2W_1	$LP(2)S_5 \rightarrow \sigma^*_{H10 - S11}$	3.43	0.45	0.035
	$LP(1)O_7 \rightarrow \sigma^*_{C1 - H4}$	0.12	0.72	0.008
	$LP(2)O_7 \rightarrow \sigma^*_{S5 - H6}$	0.96	0.82	0.025
	$LP(2)S_{11} \rightarrow \sigma^*_{O7 - H8}$	7.39	0.68	0.064
	$LP(2)S_{11} \rightarrow \sigma^*_{O7 - H9}$	0.07	0.70	0.006
M_4	$LP(2)S_7 \rightarrow \sigma^*_{H2-S6}$	3.72	0.45	0.037
	$LP(2)S_6 \rightarrow \sigma^*_{H3-S5}$	3.70	0.45	0.037
	$LP(2)S_5 \rightarrow \sigma^*_{H4-S8}$	3.70	0.45	0.037
	$LP(2)S_8 \rightarrow \sigma^*_{H1-S7}$	3.69	0.45	0.037
W_4	$LP(2)O_1 \rightarrow \sigma^*_{O4 - H5}$	17.18	0.90	0.111
	$LP(2)O_4 \rightarrow \sigma^*_{O7 - H8}$	17.17	0.90	0.111
	$LP(2)O_7 \rightarrow \sigma^*_{O10 - H11}$	17.18	0.90	0.111
	$LP(2)O_{10} \rightarrow \sigma^*_{O1 - H3}$	17.18	0.90	0.111
M_1W_3	$LP(2)S_5 \rightarrow \sigma^*_{O10 - H11}$	12.83	0.67	0.083
	$LP(2)O_7 \rightarrow \sigma^*_{O13 - H14}$	13.92	0.93	0.102
	$LP(2)O_{10} \rightarrow \sigma^*_{O7 - H9}$	15.12	0.92	0.106
	$LP(2)O_{13} \rightarrow \sigma^*_{S5 - H6}$	6.19	0.64	0.056
M_2W_2	$LP(2)S_5 \rightarrow \sigma^*_{H10 - S14}$	5.27	0.45	0.044
	$LP(2)O_7 \rightarrow \sigma^*_{O11-H12}$	11.24	0.92	0.091
	$LP(2)S_{14} \rightarrow \sigma^*_{O7-H9}$	12.63	0.67	0.083
	$LP(2)O_{11} \rightarrow \sigma^*_{S5 -H6}$	4.03	0.63	0.045
M_2W_2 anti	$LP(2)S_5 \rightarrow \sigma^*_{O8 - H9}$	10.26	0.68	0.075
	$LP(2)S_{14} \rightarrow \sigma^*_{O11 - H12}$	10.26	0.68	0.075
	$LP(2)O_8 \rightarrow \sigma^*_{H7 - S14}$	5.67	0.67	0.055
	$LP(2)O_{11} \rightarrow \sigma^*_{S5 - H6}$	5.67	0.67	0.055
M_3W_1	$LP(2)S_5 \rightarrow \sigma^*_{H10-S12}$	5.44	0.45	0.044
	$LP(2)S_{17} \rightarrow \sigma^*_{S5-H6}$	3.64	0.45	0.036
	$LP(2)S_{12} \rightarrow \sigma^*_{O7-H9}$	9.11	0.69	0.071
	$LP(2)O_7 \rightarrow \sigma^*_{H11-S17}$	1.51	0.81	0.031

Methanethiol and methanol differ only by one atom and the electronegativity difference between oxygen and sulfur is very small (0.86) on the Pauling scale. This is one of the dominating factors regarding hydrogen bonding, and this effect is highly significant and conspicuous in O-H---S, S-H---O, and O-H---O interactions which were well studied by both experiment and theory [26], [166]. Table 5.9 reveals different values of the interaction energy

for W_n cluster even at same level of theory. Trend observed in the case of methanol–water complexes [136] was also found to be similar for the M_mW_n clusters as well.

Table 5.9 Comparison of interaction energy[$] (kcal/mol) and bond length for M_mW_n cluster with its homologous menthanol-water system at B3LYP/6-311++G(d,p) level of theory.

System	M_mW_n (this work)	(MOH-H_2O) @ Mondal et al.[136]
M_2	-2.65	-5.29
W_2	**-5.83 (1.956 Å)**	**-5.07 (1.949 Å)**
M_1W_1	-4.36	-4.89/-5.45
M_3	-5.62	-16.50
W_3	**-17.32 (1.901-1.924 Å)**	**-15.94 (1.911-1.941 Å)**
M_1W_2	-12.73	-16.02
M_2W_1	-8.47	-16.30/-16.57
M_4	-9.68	-29.21
W_4	**-30.78 (1.770 Å)**	**-28.59 (1.791 Å)**
M_1W_3	-23.68	-28.73
M_2W_2	-18.23	-28.89
M_2W_2 anti	-17.07	-28.91
M_3W_1	-13.19	-29.03
$ Note: $IE = (E_{cluster} - (\sum_{m=1}^{4} M_m + \sum_{n=1}^{4} W_n))$		

From above Table we see that our considered water clusters are much stable than the Mondal et al.'s clusters. Hydrogen bond distance corresponding to O-H---O interaction is also larger than the Mondal et al.'s values [136] in the dimeric system but comparable for trimer and tetrameric system.

5.4 Conclusion

Strength and nature of SCHB involved in the M_mW_n clusters were studied by applying quantum chemical calculation. Optimized geometries were free from imaginary frequency and the normal modes of vibrations matched exceedingly well with earlier reported experimental values. The computed interaction energy, geometrical parameters, and vibrational frequencies display a trend that is similar to its homologous methanol-water cluster. With increase of cluster size, length of S-H---S, O-H---S, S-H---O, and O-H---O interactions decreased, and the corresponding interaction energies increased. Herein, sulfur atom acts as both a donor and acceptor of hydrogen bond in all the cluster systems. Interaction energy corresponding to O-H---S hydrogen bond was larger than the S-H---O hydrogen bond. Local energy decomposition module suggested electrostatic energy to be to dominant contributor to the interaction energy in all the instances of SCHBs.